I.A.U
Karaj branch

Journal of
A p p l ied
C hemical
R esearch
jacr.kiau.ac.ir

Journal of Applied Chemical Research, 15, 2, 31-45(2021)

Corrosion Inhibition of AISI 304 Stainless Steel using Zinc Nitride Coating

Fatemeh Abdi

Department of Engineering Sciences, Faculty of Advanced Technologies, University of Mohaghegh Ardabili, Namin, Iran

(Received 23Aug. 2020; Final revised received 14Nov.2020)

Abstract

The corrosion behavior of Zn/ (AISI304) annealed at different temperatures with flow of nitrogen gas was investigated in the 3.5%NaCl solution. Crystallography structure of the samples was analyzed using X-ray diffraction (XRD) pattern. The results showed that with increasing annealing temperature, the intensities of oxide and nitride phases were increased. Surface morphology of the samples was studied using atomic force microscope (AFM) before corrosion tests. AFM results showed that by increasing annealing temperature, grains become greater that may be the result of heat accumulation, causing higher rate of diffusion in the sample. Electrochemical Impedance spectroscopy (EIS) and Polarization tests were carried out for corrosion resistance investigation of the produced samples. The corrosion results revealed that highest corrosion resistance was achieved for the sample at the highest annealing temperature. For more in depth analysis, the equivalent circuit of samples was obtained, using the EIS data. Finally, the surface of the corroded samples was observed using scanning electron microscopy (SEM).

***Keywords*:** Corrosion, AISI304 Stainless Steel, Zn_3N_2, Polarization, EIS, Equivalent circuit.

.

[*]***Corresponding author:*** *Fatemeh Abdi, Department of Engineering Sciences, Faculty of Advanced Technologies, University of Mohaghegh Ardabili, Namin, Iran. E-mail: Email: F.Abdi@uma.ac.ir.*

.

Introduction

Stainless steel (e.g., types AISI 304 and AISI 316) has many applications in industry and technology (such as oil and gas industry, offshore platforms, nuclear reactors, aerospace) due to its good mechanical properties and good corrosion resistance. [1,2]. However, However, this substance does not have much resistance in the environments containing aggressive ions such as $Cl^-$and S^{-2}, especially at high temperatures and environments with very high or low pHs[3-5]. Therefore, improving the resistance of this highly used material against corrosion in different environments is very necessary. Variation of the ratio of different elements in the structure of stainless steels results in different corrosion behavior in each corroding medium [6, 7]. The corrosion behavior of AISI 304 and AISI 316 types of stainless steels for various applications is evaluated in different studies, using different methods namely ion implantation [8], sol gel deposition [9,10], chemical deposition [11], physical deposition[12], arc-ion plating [13], chemical conversion layers of cerium [14] chromium [15] or other elements, high-velocity oxy-fuel spray [16], plasma-nitriding [17], and lately Atomic Layer Deposition (ALD) [18–20]

Physical vapor deposition Cause numerous microscopic defects in the structure of the coated layer and this make the film prone to corrosion attack [21-23]. In other word, the imperfections, pinholes and cracks can be the starting points for the localized corrosion. Researchers have improved the quality of the coatings, using different methods to reduce the amount of these imperfections. Increasing the number coating layers [24-32], increases the number of interfaces, is a common solution to modify the microstructure of the coating layer the other work that can be used for defect reduction of coating is post annealing of the structure in the flow of gases. In recent years, transition metal nitrides such as NiN and TiN films have been identified as the promising coatings to corrosion protection [33-40]. In this work we have studiedthe corrosion resistance of ZnN thin film on the AISI 304 stainless steel in 0.6 M (3.5 %) NaCl solution for this purpose, a thin layer of zinc was deposited on steel substrates. Then the samples were annealed within nitrogen flux at different temperatures for nitriding. After preparing the samples, annealing temperature effect on structure, morphology and corrosion resistant of the samples was investigated.

Experimental

After cutting the substrates to the desired size of (20 × 20 × 1 mm), the polyethylene sheet that was covered the surface of the stainless steel for scratching protection, was removed by soaking in ethanol. The chemical composition of the stainless steel used in this work is given in Table 1.

Table 1. Chemical composition of AISI 304 type stainless steelused in this work. .

Element (wt. %)

Mn	Ni	Cr	Si	C	P	S
1.62	8.00	18.34	0.34	0.07	0.043	0.03

Prior to deposition all substrates were ultrasonically cleaned in heated acetone then ethanol.The substrates were glued to the substrate holder with vacuum adhesive. Zinc with a purity of 99.98% was considered as the coating layer material. An Edwards (Edwards E19 A3) coating plant with a base pressure of 2×10^{-7} mbar was usedand the deposition was performed at room temperature by an electron gun. Thus, 100 nm of Zn was formed on steel substrates. Since small crucibles are used in this experiment (6 mm in diameter) they can be considered as point sources and it can be assumed that they should provide similar evaporation condition (flux) to all substrates and the single layer of the same thickness can be obtained for all samples. The film thickness was controlled by a quartz crystal deposition rate controller (Sigma instrument, SQM – 160, USA) positioned close to the substrates. The nominal deposition rate for Zn was 0.5 $Å s^{-1}$.Postannealingof Zn/(AISI 304)samples were performed at three different temperatures of 400K, 500K and 600K in nitrogen environment with a flow rate of 500 sccm, using a cylindrical horizontal quartz tube furnace (Exciton, 1200-30/6, T.H, Iran equipped to Shinko temperature programmable controller – PCD 33A). The annealing procedure took place in three steps as:

1) two hours to reach the set annealing temperature

2) Samples were kept at pre-set annealing temperature for seven hours

3) twelve hours cooling temperature

The cooling procedure of the samples took place inside the quartz tube of the furnace with the same flow of nitrogen used during annealing. Crystallographic structure of these films was obtained using a STOE model STADI MP Diffractometer, Germany (CuK_{α}radiation) with a step size of 0.01º and count time of 1.0s per step, while the surface physical morphology/nano structure and roughness was obtained by means of AFM (Nt-mdt scanning probe microscope, BL022, Russia; with low stress silicon nitride tip of less than 200 Å radius and tip opening of 18°) analysis and scanning electron microscope (SEM: LEO 440i, England). Root mean square (rms) andaverage surface roughness as well as average grain size of the samples was obtained from the 2D AFM images using Nova and JMicroVision Codes, respectively. The electrochemical test of the samples was performed using potentiodynamic method with a potentiostat coupled to PC (273A, EG & G, USA). In order to carry out this analysis only an area of 1.0 ± 0.05 cm^2 was exposed to the 3.5%NaCl solution.

The polarization potential was applied via a copper wire contacted to the back side of the sample in the fixture, while a saturated calomel reference electrode (SCE) and a platinum counter electrode were used in a three electrode setup.The potential was swept with a rate of 1 mV $s^{-1}$to cover a range of about 1V for each sample, starting from -400 mV vs. open circuit potential. All measurements were performed at 298 K.All of the potentials presented in this work are as a function of SCE. An initial delay of one hour for the samples to reach a steady state condition was considered before electrochemical impedance spectroscopy (EIS) and polarization tests.

The corrosion current density j_{corr} and the corrosion potential E_{corr} were calculated from the Tafel extrapolation of polarization curves of semi-logarithmic plot using the method prescribed in [41]. In order to make an accurate Tafel extrapolation we started our extrapolation at least 50-100 mV away from Ecorr, while as prescribed in the literature [42, 43], our polarization curves also containat least one linear (semi-logarithmic) scale (see for example Fig. 2) which facilitates accurate extrapolation.

The electrochemical impedance spectroscopy (EIS) measurements were also performed using the above mentioned cell used for corrosion test and the equipment used in the polarization test. Impedance values were recorded in the frequency range of 100 kHz to 100 mHz. The voltage amplitude was 10 mV with respect to the open circuit potential. The analysis of the impedance spectra was performed using Zview software and the equivalent circuit fitted to the experimental data was obtained.

Results and discussion

AFM analysis

Atomic force microscopy analysis was used to examine surface morphology of the samples. The difference in the surface morphology of samples annealed at different temperatures is displayed in Figure 1.Table 2 summarizes the average grain size (D_{AFM}), average surface roughness (Rave) and the root mean square roughness (Rms)values deduced from the AFM analyses. The results show, the sample annealed at 400 K has grains of 95 nm in size, increasing the annealing temperature to 500K, increase the average grain size (i.e., 110 nm). Further increase of the annealing temperature to 600 K produced larger grains that could be due to the increased diffusion rate. By increasing annealing temperature, the number of grain boundaries was decreased. It can be observed in Table 2 that the film surface roughness increases with the annealing temperature, as it is expected from the above discussion about the variation of the average grain size that are due to the increased diffusion effect.

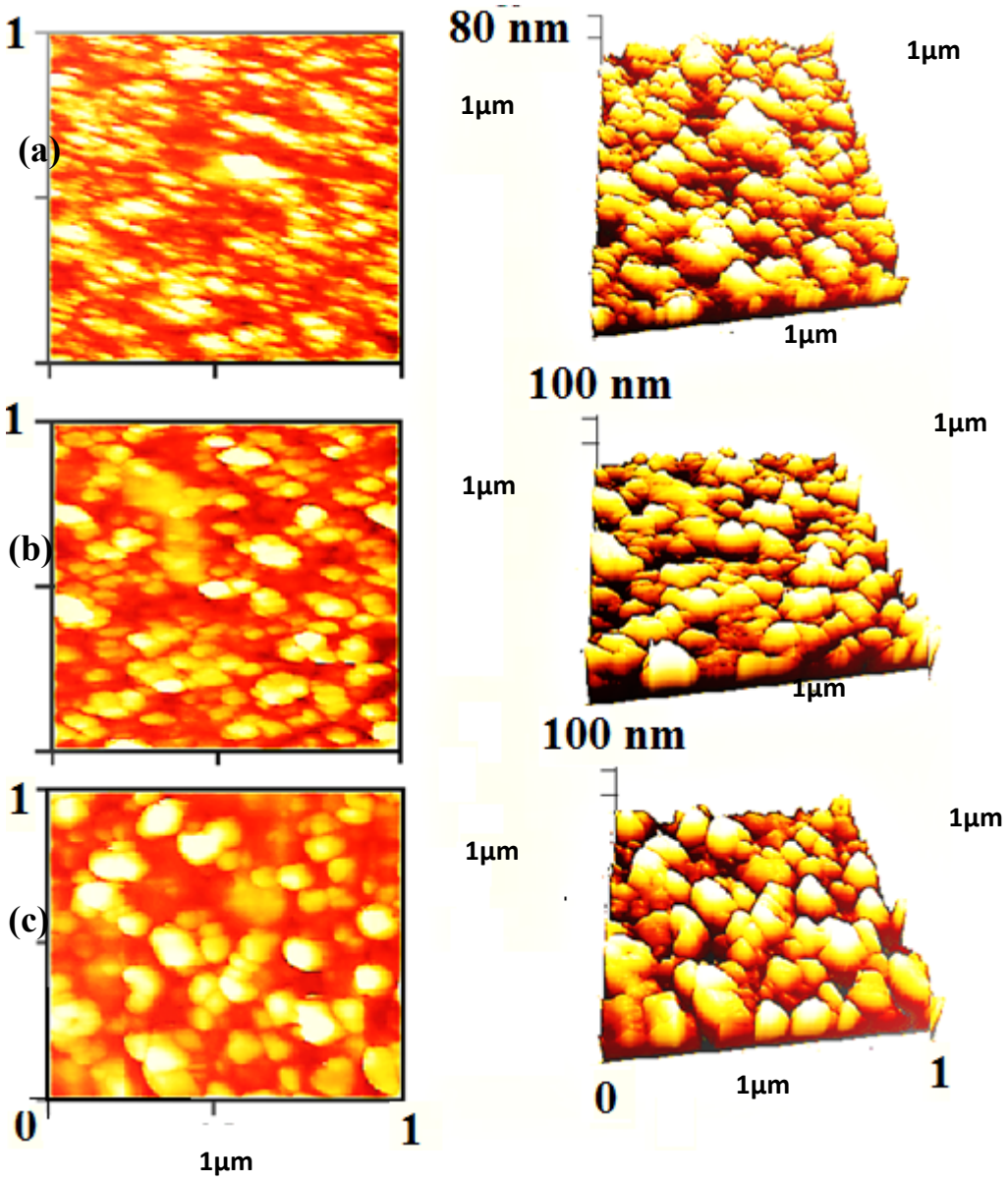

Figure 1. 2D and 3D AFM images of the (ZnN/(AISI 304)) samples annealed at different temperatures with different average grain sizes; a) 400 K, b) 500 K, c) 600K.

Table 2. Details of experimental results for AISI 304 stainless steel and Zn/(AISI 304) at different annealing temperatures.

***T*(K)**	R_{ave} **(nm)**	***Rms*** **(nm)**	D_{AFM} **(nm)**	**Corrosion current density (μA cm^{-2})**	**Corrosion potential (V(SCE))**
Untreated	8.6	10.9	-	131.82	-0.50
400	16	20.6	95	17.02	-0.31
500	20	26.2	110	2.09	-0.28
600	25	33.7	130	1.15	-0.15

Crystal structure analysis

Figure2 shows XRD patterns of the ZnN/(AISI 304) coatings annealed at different temperatures and the AISI 304 stainless steel as a reference. The original structures of the steel substrates comprised of just austenite phases detectable by X-ray and it is clear that the substrate presents a single phase γ-Fe with sharp peaks correspond to γ–Fe(111), γ–Fe(200), γ–Fe(220) and γ–Fe(311) at 2θ = 43.67°, 50.85°, 74.81° and 90.81° [51-53]. Examination of the XRD pattern of the sample annealed at 400 K reveals one Zn3N2 peak at 2θ = 47.46º corresponding to Zn3N2 (431) and three Zn peaks at 2θ = 36.18º , 44.18º and 54.08º corresponding to Zn(002) , Zn(101) and Zn(102) lines, respectively while the intensity of the diffraction lines of stainless steel are reduced.

The intensities of Zn diffraction lines are significantly decreased when the annealing temperature is increased to 500 K and we can see formation of oxide and nitride phases in this temperature. Diffraction lines of Zn_3N_2 (321), Zn_3N_2 (400), Zn_3N_2 (431), Zn_3N_2 (622), ZnO (110) appeared at 2θ = 34.3°, 36.57º, 47.46º, 63.27º and 56.57º respectively. Intensity increasing of the line at 2θ = 44.18º attributed to the formation of ZnO (101) phase in these temperature.

At 600 K annealing temperature, the intensity of Zn3N2 lines are increased and ZnO peaks intensities are decreased while two Zn peaks are disappeared.

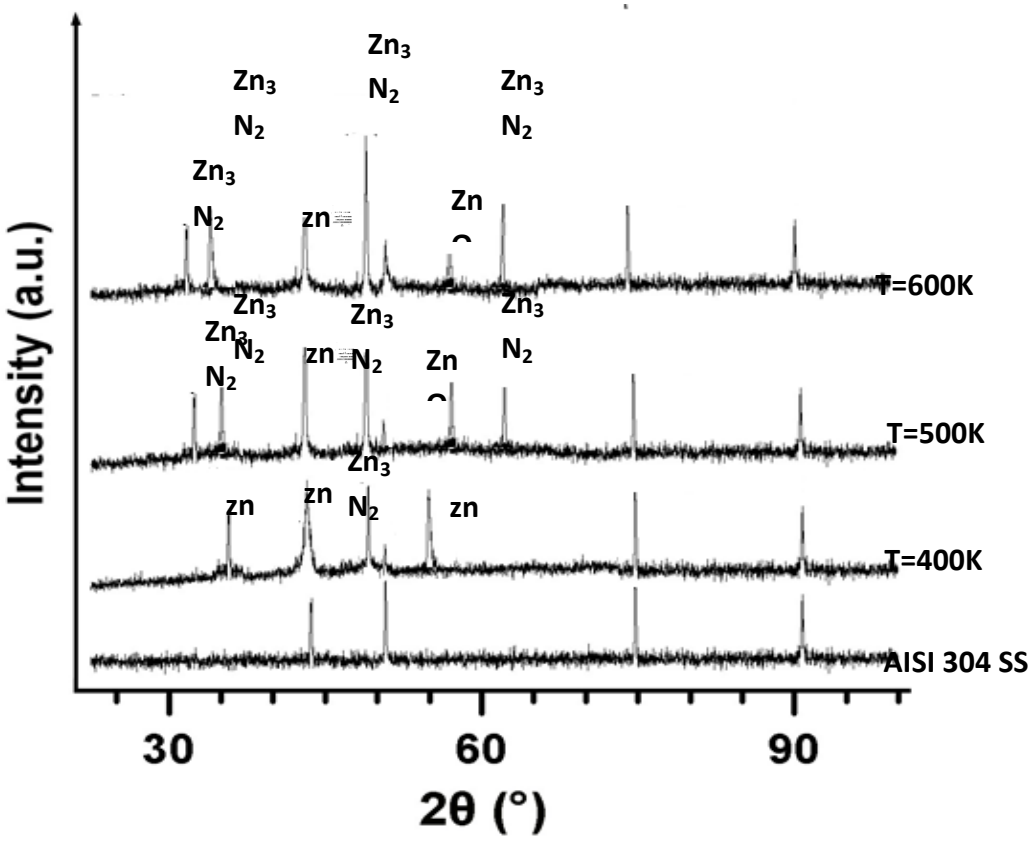

Figure 2. XRD spectra of samples annealed at different temperatures.

Electrochemical analyses

The potentiodynamic polarization curves of the ZnN/ (AISI 304)annealed at different temperatures in 3.5% NaCl solution are shown in Figure3 .The polarization curve of the AISI 304 stainless steel substrate is also given in the figure for comparison. The values of the corrosion potential and the corrosion current density are derived from the polarization curves by Tafel extrapolation for these samples [41-53].Results of the corrosion current density and the corrosion potential of the samples are given in columns 5 and 6 of Tables 2.

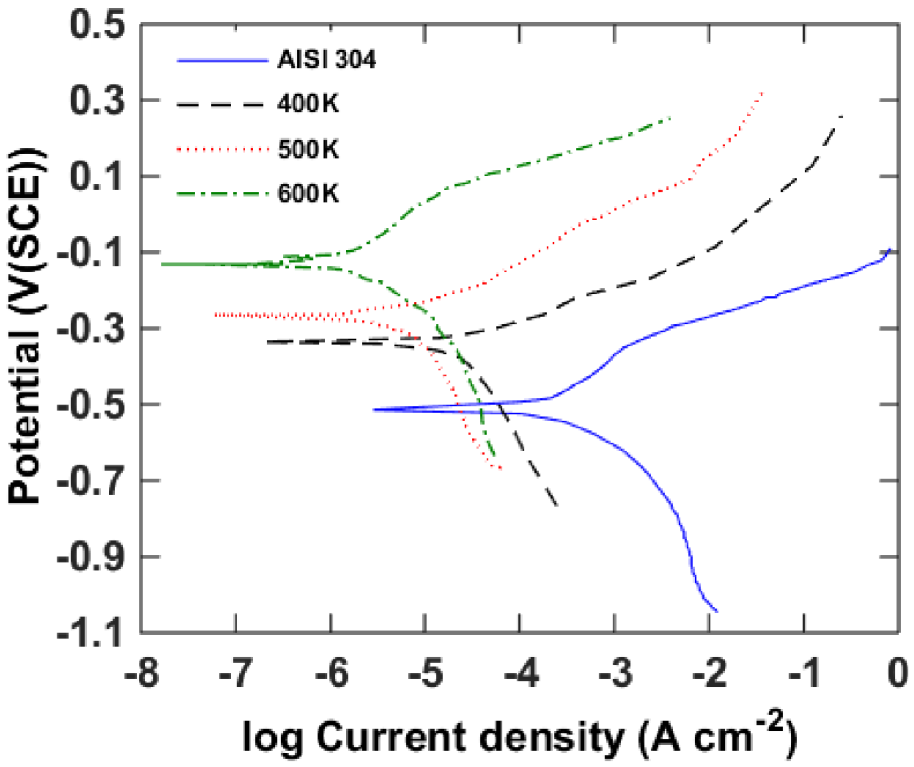

Figure 3. Potentiodynamic polarization curves of the AISI 304 stainless steel, ZnN/(AISI.

It is a clear that the sample annealed at 600 K has the lowest corrosion current and the highest corrosion potential. The values of corrosion current density for the samples annealed at lower temperatures are higher than that for the sample annealed at 600 K. The highest value of the corrosion current density is related to the lower annealing temperature of 400 K. Hence, it is expected that this sample shows the lowest corrosion resistance in the corroding medium (3.5% NaCl solution).This could be due to formation of the oxide and nitride phases at high temperatures. By increasing annealing temperature from 400 K to 500K, ZnO and Zn_3N_2 phases are formed and this oxide and nitride phases can act as a barrier against aggressive ions. Because of high intensity of the nitride phases at 600 K annealing temperature, corrosion resistant of thissample is the highest.

When the films are exposed to the corrosive medium, the solution reaches the defects such as cracks and pores in the coating, then difference in the binding energy and the chemical composition between the coating matrix and the substrate can produce galvanic corrosion cell [44]. Therefore, higher grain size also acts as a buffer against the corroding medium should show a better corrosion behavior as observed in Fig 3 and Table2.One may expect to observe pitting or passive state in the AISI 304 stainless steel and single layer films deposited on this substrate in the chloride solution in this work. However, because of the following reasons we may point out that this is not the case or is

minimized. With regard to the stainless steel itself, it should be mentioned that in fact passivation is hindered by the complexing attitude of Cl^- ion towards Fe^{2+} and Cr^{3+}; for this reason, potential tends to decrease. As pointed out in [45] and in [46] in chloride containing electrolytes passivation of stainless steels is inhibited or the passive film is readily dissolved. Hence, we could not observe passivation state for the AISI 304 stainless steel used in this work.On the other hand, as pointed out in the following references nitrogen increases the grain boundary resistance [47-49]and nitrogen in the austenitic stainless steel increases its strength [50]and enhances its crevice and inter-granular corrosion in some media [51-54], while nitrogen alloying addition, in particular reduces the pitting susceptibility of the stainless steel [37].

The impedance spectroscopy of the samples was carried out to determine the complex frequency-dependent impedance $Z(\omega) = Z' + iZ''(\omega)$, of all samples. Plotting for a simple RC circuit, the negative imaginary part of $Z(\omega)$, $-\mathrm{Im}Z(\omega)$, as a function of the real part, $\mathrm{Re}Z(\omega)$, would usually result in semicircle with a diameter *R* (Nyquist plot [55]) and its centre at the $\mathrm{Re}Z(\omega)$axis, at a distance of *R/2* from the origin. The presence of any additional resistance R_c due to contacts will shift the center of the semicircle by R_c to higher values. The diameter of such semicircle will provide the value for *R* and the value of *C* can be obtained from the relation $C = \frac{1}{(R\omega_a)}$, where $R\omega_a$ is the value of ω at the apex of the semicircle.

Figure 4 show the Nyquist plots of the ZnN/ (AISI 304) annealed at different temperatures and the bare stainless steel in 3.5% NaCl solution, respectively. Each sample was left in the corroding medium for 1 hour before taking measurements for the Nyquist plot.It is clear from the figure that with increasing annealing temperature, electrical impedance and corrosion resistance increase.

Fig. 5 shows the equivalent circuit used to simulate the EIS data for the systems. In this equivalent circuit, R_s is the solution resistance, R_p is polarization resistance and it is inversely proportional to the corrosion rate [56], C_{coat} represents the film capacitance. Due to the in homogeneity structure of thin films and due to the surface roughness of the coating, C_{coat} is not an ideal capacitor.

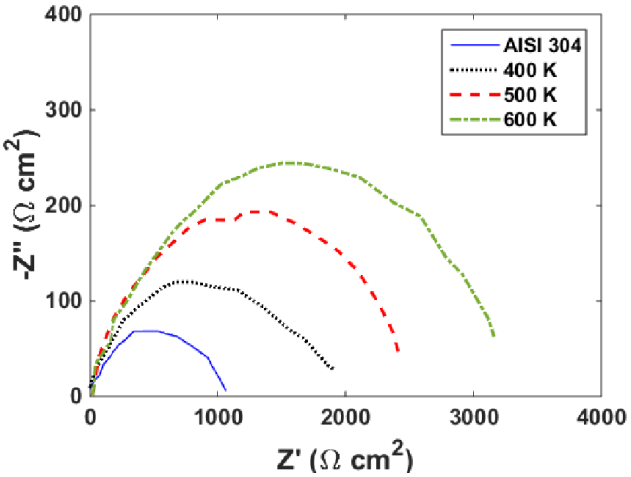

Figure 4. Experimental Nyquist diagrams for the stainless steel, the (ZnN/(AISI 304)) (a), and samples in 3.5% NaCl solution annealed at different temperatures.

Considering the experimental results and the equivalent circuit, the fitted values for the equivalent circuit components are given in Table 3. As mentioned above the polarization resistance $R_p$is inversely proportional to the corrosion rate and the values obtained for R_p in Table 3 show that, R_p value is lowest for AISI 304 . By increasing annealing temperature, the corrosion resistance has increased and the sample annealed at 600 K has the highest corrosion resistance. This is consistent with the results obtained for corrosion current density (lowest value) discussed above. The formation of oxide and nitride phases at 500 K and 600K temperatures and increasing of nitride phase intensity at 600 K is the Cause of corrosion resistant increasing for this sample.

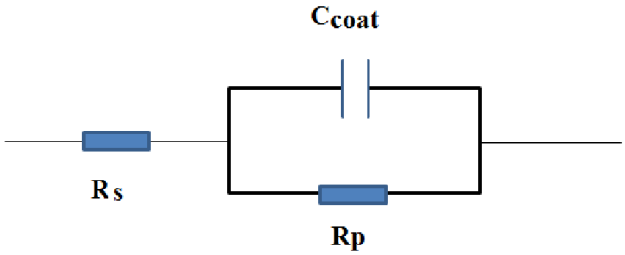

Figure 5. Electrical equivalent circuit of the experimental EIS data of all samples. Rs: solution resistance; Rp: polarization resistance; Ccoat: coating capacitance.

It is well known that during the deposition process, oxygen and other contaminants accumulate at grain boundaries and may cause the formation of growth steps [57-59].Henceafter deposition of Zn(which is a highly reactive material)itcan react with oxygen and form different oxides with different stochiometry and phases [60, 61] and can increase corrosion resistance and reduce corrosion rate.

Table 3. Electrochemical parameters of AISI 304 stainless steel, Zn/(AISI 304)single layer samples annealed at different temperatures subjected to corrosion test in 0.6 M NaCl, obtained from fitting of EIS spectra by equivalent circuit.

***T*(K)**	R_s(Ω cm^2)	R_p (kΩ cm^2)	C_{coat} (mF cm^{-2})	α
Untreated	20.8	0.1126	1.53	0.95
400	19.2	1.98	0.522	0.87
500	22.2	2.43	0.358	0.93
600	20.19	3.23	0.22	0.92

SEM analysis

Figures 6 (a-d) show the surface morphology of the corroded samples annealed at different temperatures after respectively. It is obvious from the figure that uncoated AISI 304 stainless steel substrate shows very obvious signs of corrosion attack on the surface of the sample (Figure 6 (a)). SEM images of nitride samples exhibit different morphologies with various types and sizes of corrosion effect such as pits and dissolutions. In Figure 6 it can be clearly seen that the sample annealed at 600 K (Figure 6(d)) shows the least amount of the above mentioned corrosion effects as it has also given the best results for the potentiodynamic test (Table 2). On the surface of samples annealed at 400 one may distinguish pits and peel offs of Zinc nitride layer and deeper attacks of the corroding medium into the AISI 304 substrates (Figure 6(b)) while small pits or imperfections have caused an almost uniform distribution of corrosion on the surface of the sample annealed at 500 K (Figure 6(c)).

The high corrosion inhibition of the samples annealed at 600 K is directly related to the nanostructure of these films and their crystallographical composition discussed in Section 3.2 (AFM results) and Section 3.1 (XRD results). The XRD results showed that the highest intensity of the nitride phase is formed at a temperature of 600 K. This increasing of nitride phase intensity, increase the grain boundary resistance [51]. Nitrogen can also act as a local-buffer at the film/substrate interface or exert its beneficial effects by improving the bonding at the metal oxide interface (by creating a barrier layer) [52-56]. Hence, it can be suggested that the increased intensities of nitride peaks in the samples annealed at 600 K is responsible for the increased corrosion resistance of these samples. However, the AFM results in Figure 3 also show the lowest grain boundaries (large grains have low grains boundaries).

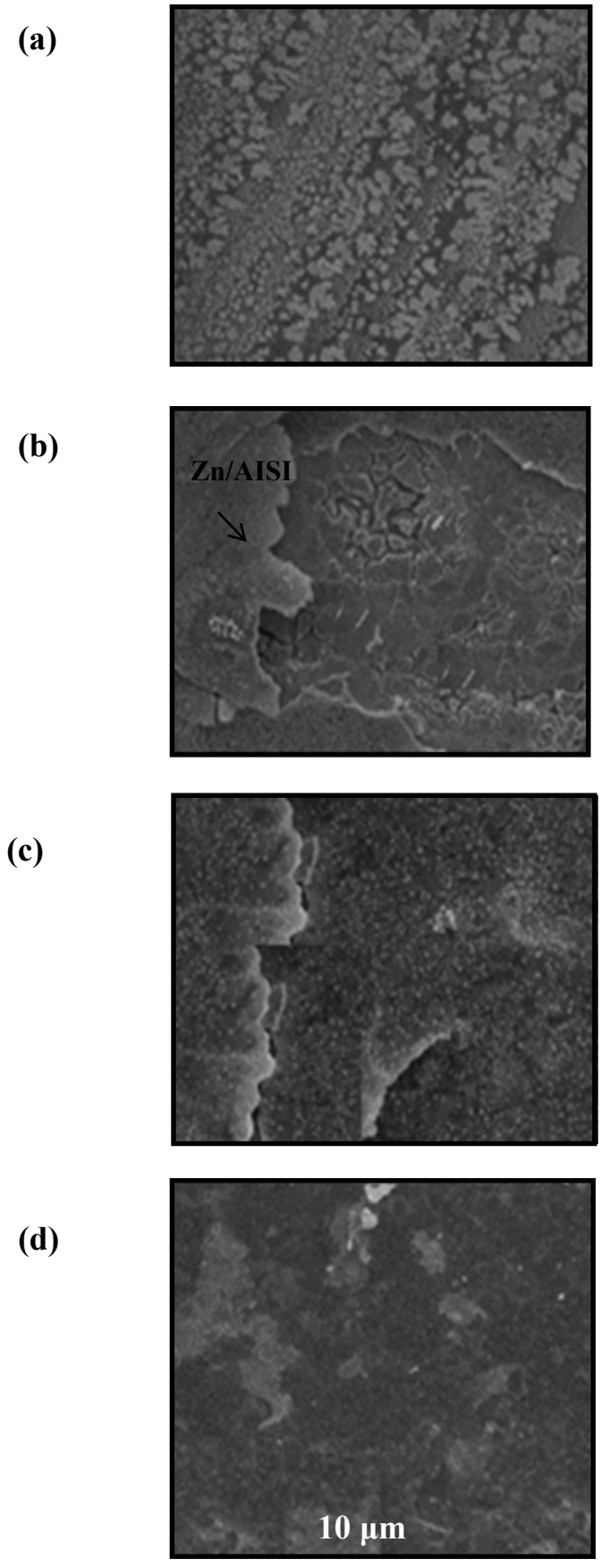

Figure 6.SEM micrograph of the AISI 304 stainless steel and the single layer (ZnN/(AISI 304)) samples annealed at different temperatures after corrosion test in 3.5% NaCl solution; a) AISI 304, b) 400 K, c) 500 K, d) 600 K.

Conclusions

In this work we have shown that coating of Zn on the surface of the AISI304 stainless steel makes a substantial improvement on its corrosion resistance in the 0.6 M NaCl corroding medium. The results show that annealing temperature increasing, corrosion resistance of the sample in the 0.6 M NaCl solution. In addition, it is also found that the surface morphology has also the same effect on the corrosion resistance: the sample with larger grains, show higher resistance in the corroding medium. It is observed that at high annealing temperatures due to increased diffusion effect large grains are formed. The better corrosion resistance results obtained for the samples annealed at high temperatures, may be related to the increasing of oxide and nitride phases intensity and reduction of the film grain boundaries. Equivalent circuit parameters showed that capacitance of capacitor decreases and electrical resistances increases by increasing annealing temperature which leads to improvement of corrosion resistance of the sample.

Acknowledgments

This work was carried out with the support of the University of Mohaghegh Ardabili.

References:

[1] N.R. Baddoo, *Journal of Constructional Steel Research*, 64, 1199 (2008).

[2] K.M. Perkins, M.R. Bache*, Int. J. Fatigue*,22, 1499(2005).

[3] K. Asami, K. Hashimoto, *Corros. Sci*.,45,2263 (2003).

[4] H. Savaloni, M. Habibi, *Applied Surface Science,* 258, 103 (2011).

[5] S.E. Ziemniak, M. Hanson, *Corros. Sci*.,44,2209 (2002).

[6] V.H.V. Sarmento, M.G. Schiavetto, P. Hammer, A.V. Benedetti, C.S. Fugivara, P.H. Suegama, S.H. Pulcinelli, C.V. Santilli, *Surf. Coat. Technol*., 204, 2689(2010).

[7] R. Di Maggio, L. Fedrizzi, S. Rossi, P. Scardi, *Thin Solid Films*, 286, 127(1996)

[8] H. Zhang, Y.L. Zhao, Z.D. Jiang, *Mater. Lett*., 59,3370 (2005).

[9] D.H. Mesa, A. Toro, A. Sinatora, A.P. Tschiptschin, *Wear*, 255,139 (2003).

[10] D. Pech, P. Steyer, J. P. Millet*, Corros. Sci.*, 50, 1492 (2008).

[11] P. Misaelides, A. Hatzidimitriou, F. Noli, A.D. Pogrebnjak, Y.N. Tyurin, S. Kosionidis, *Surf. Coat. Technol*., 180,290 (2004).

[12] C. Liu, G. Lin, D. Yang, M. Qi, *Surf. Coat. Technol*., 200, 4011(2006).

[13] C. Wang, F. Jiang, F. Wang, *Corros. Sci*., 46 ,75(2004)

[14] C.R. Tomachuk, C.I. Elsner, A.R. Di Sarli, O.B. Ferraz, *Mater. Chem. Phys*., 119,19(2010).

[15] D. Pech, P. Steyer, J.P. Millet, *Corros. Sci*., 50,1492 (2008)

[16] J. Kawakita, T. Fukushima, S. Kuroda, T. Kodama, *Corros. Sci*., 44, 2561 (2002).

[17] C.X. Li, T. Bell, *Corros. Sci*., 48,2036(2006).

[18] B. Díaz, J. Światowska, V. Maurice, A. Seyeux, B. Normand, E. Härkönen, M. Ritala, P. Marcus, *Electrochem. Acta*, 29, 5(2011),

[19] E. Marin, A. Lanzutti, L. Guzman, L. Fedrizzi, *J. Coat. Technol. Res*., 8, 9372(1998).

[20] C.X. Shan, X. Hou, K.-L. Choy, *Surf. Coat. Technol*., 202, 2399(2008).

[21] H-P. Feng, C-H. Hsu, J-K. Lu, Y-H. Shy, *Mater. Sci. Eng. A*,347, 123(2003)

[22] M. Bromark, M. Larsson, P. Hedenqvist, S. Hogmark, *Surf. Coat. Technol*., 90, 217(1997)

[23] H. A. Jehn*, Surf. Coat. Technol*., 125, 212(2000)

[24] W.Y. Ho, C.H. Hsu, D.H. Huang, Y.C. Lin, C.L. Chang, D.Y. Wang, *Surf. Coat. Technol*., 200,1303(2005).

[25] V. K. Mittal, S. Bera, T. Saravanan, S. Sumathi, R. Krishnan, S. Rangarajan, S. Velmurugan, S. V. Narasimhan, *Thin Solid Films*, 517 ,1672(2009)

[26] L. Zeng, S. Yang, W. Zhang, Y. Guo, C. Yan, *Acta*, 55, 3376(2010)

[27] P. H. Suegama, H. G. demelo, A. A. C. Recco, A. P. Tschiptschin, I. V. Aoki, *Surf. Coat. Technol*., 202, 2850(2008).

[28] M. Fenker, M. Balzer, H. Kappl, *Thin Solid Films*, 515, 27(2006).

[29] L. A. S. Ries, D. S. Azambuja, I. J. R. Baumvol, *Surf. Coat. Technol*., 89 ,114(1997)

[30] Y.S. Choi, Y.H. Yoo, J.G. Kim, S.H. Kim, *Surf. Coat. Technol*., 201, 3775(2006)

[31] E. Bemporad, C. Pecchio, S. De Rossi, F. Carassiti, *Surf. Coat. Technol*., 188,319(2004).

[32] C. Mendibide, P. Steyer, J.P. Millet, *Surf. Coat. Technol*., 200, 109(2005).

[33] E. Menthe, K.T. Rie, *Surf. Coat. Technol*., 116, 199(1999).

[34] V. Muthupandi, P. Bala Srinivasan, V. Shankar, S. K. Seshadri, S. Sundaresan, *Mater. Lett.,* 59, 2305(2005).

[35] J. Baranowska, B. Arnold, *Surf. Coat. Technol*., 200, 6623(2006)

[36] M. Yatsuzuka, S. Miki, R. Morita, K. Azuma, E. Fujiwara, H. Uchida, *Vacuum*, 59,330(2000)

[37] L. Nosei, M. Avalos, B. J. Gomez, L. Nachez, J. Feugeas, *Thin Solid Films*, 468 134(2004)

[38] C. Garcia, F. Martin , Y. Blanco, M. P. de Tiedra, M. L. Aparicio, *Corros. Sci*., 51, 76(2009)

[39] J. H. Potgieter, P. A. Olubambi, L. Cornish, C. N. Machio, E. M. Sherif, *Corros. Sci.*, 50,2572(2008).

[40] M. F. Montemor, A. M. P. Simoes, M. G. S. Ferreira, M. Da Cunha Belo, *Corros. Sci*., 41, 17(1999)

[41] E. E. Stansbury, R. A. Buchanan ,Fundamentals of Electrochemical Corrosion, ASM, Ohio (2000).

[42] E. Poorqasemi, O. Abootalebi, M. Peikari, F. Haqdar, *Corros. Sci*., 51, 1043(2009)

[43] R. Kelly, J. R. Scully, D. Shoesmith, R. G. Buchheit, Electrochemical techniques in corrosion science and engineering, Dekker, New York (2002).

[44] S. H. Ahn, J. H. Lee, J. G. Kim, J. G. Han, *Surf. Coat. Technol*. 177, 638(2004).

[45] L. L. Shreir, R. A. Jarman ,G. T. Burstein, Corrosion, Butterworth-Heineman, Oxford(2000).

[46] L. Ceschini, C. Chiavari, E. Lanzoni, C. Martini, *Materials and Design*, 38, 154(2012)

[47] B. Chico, L. Martinez, F.J. PerezAppl. *Surf. Sci*., 243, 409(2005).

[48] R.F.A. Jargelius-Pettersso, *Corrosion Science*, 41, 1639(1999)

[49] V. Singh, K. Marchev, C.V. Cooper, E.I. Meletis, *Surface and Coatings Technology*, 160, 249(2002)

[50] C.M. Tseng, H.Y. Liou, W.T. Tsai, *Mater. Sci. Eng*. A, 344, 190(2003)

[51] H. Yashiro, D. Hirayasu, N. Kumagai, *ISIJ Int*., 42,1477(2002)

[52] G. C. Palit, V. Kain, H. S. Gadiyar, *Corrosion*, 49, 979(1993)

[53] Y. C. Lu, R. Bandy, C. R. Clayton, R. C. Newman, *J. Electrochem. Soc*.,130, 1774(1983)

[54] C-O. A. Olsson, *Corros. Sci*., 37, 467(1995)

[55] S. Ningshen, U. Kamachi Mudali, V. K. Mittal, H. S. Khatak, *Corros.Sci*., 49, 481(2007).

[56] H-B. Li, Z-H. Jiang, Y. Yang, Y. Cao, Z-R. Zhang, *Int. J. Miner. Metall. Mater*.,16,517(2009).